Panel method control in 3-D hyberbolic grid generation

M H L Hounjet

National Aerospace Laboratory (NLR), Anthony Fokkerweg 2,
1059 CM Amsterdam, The Netherlands

A method is presented for the generation of OH type grids about transport type aircraft. The method combines a hyperbolic grid generation scheme with source terms obtained with a panel method in such a way that OH type grids around fairly complex shapes with concavities can be generated easily. The components of the method: a method to generate grids with a panel method and the hyperbolic grid generation scheme, will be described and applications will be shown.

Introduction

In the development of many modern airplanes aeroelastic analysis is required in the transonic speed range. This implies the development of computer methods to determine the unsteady transonic flow about realistic aircraft configurations which have to be executed efficiently on computational grids. The computational grids may be generated with recent sophisticated grid generation methods such as the multi-block methods and unstructured grid methods, at the expense however of a few drawbacks: 1) multi- block methods are not easy to use for 'non-grid expert' applicators and 2) multi- block and unstructured grids increase the computation time and the development time considerably. At the Unsteady Aerodynamics and Aeroelasticity Departement of NLR it was decided to develop a mono-block OH type grid generator for aeroelastic applications to complete aircraft aiming at reducing the aforementioned drawbacks. The grid generator is required in particular to generate grids of acceptable quality about concave areas such as airfoil noses and wing-fuselage junctions and should be easy to use for 'non-grid expert' applicators. Therefore a 2-D investigation was conducted of the generation of O type grids around transverse cross-sections of transport type aircraft. Research was performed on methods which generate grids in a more natural way by an evolutionary process starting at the boundaries of the configuration and constructing the grid according to an inflation analogy. The research resulted in a panel method for generating grids by solving the flow about an inflating body which was reported in [4]. During these developments the conclusion was drawn that a combination of the panel grid generator method and the hyperbolic grid generation method [1, 3] would be preferable in terms of computational cost and complexity in 3-D and this has resulted in the present method. Its essence is a hyperbolic grid generator which uses an integral method for direction and growth control in concave areas where the standard hyperbolic grid generator fails thereby reducing the effort to generate grids of acceptable quality. The paper describes this method and shows results of 2-D and 3-D examples.

Grid generation by panel method

The grid generation method starts from an initial boundary contour discretization $\vec{r}_{j,0}$ (boundary surface grid) and generates the required contours $\vec{r}_{j,k}$ denoted by the contour index k as follows:

1. From the contour grid line discretization $\vec{r}_{j,k}$ an estimate of a new contour grid line discretization $\vec{r}^{E}_{j,k+1}$ is constructed in normal direction at a distance proportional to the spacing of the contour. The estimate is improved by the following steps to avoid grid folding.

2. A panel method ([4]) for the solution of the Helmholtz eq.:
$$\phi_{yy} + \phi_{zz} - \kappa^2 \phi = 0,$$
is applied using the previous contour discretization $\vec{r}_{j,k}$ with outflow boundary conditions:
$$\vec{q}.\vec{n} = f_j = \frac{(\vec{r}^{E}_{j,k+1} - \vec{r}_{j,k}).\vec{n}_{j,k}}{\delta T} \qquad (1)$$
which simulate a potential flow about a inflating body during a uniform time increment δT. The solution provides the flow velocities $\vec{q}_{j,k+\frac{1}{2}} = \vec{\nabla}\phi$. Increasing κ reduces the global interference effect.

3. Various ways of constructing the final grid contour line discretization $\vec{r}_{j,k+1}$ in the flow direction $\vec{q}$ are possible. One way which has been applied successfully is:
$$(\vec{r}_{j,k+1} - \vec{r}_{j,k}) = (1-\beta) d\vec{r}^{E}_{j,k} + \beta \frac{d\vec{r}^{E}_{j,k}.\vec{q}_{j,k+\frac{1}{2}}}{|\, q_{j,k+\frac{1}{2}} \,|} \frac{\vec{q}_{j,k+\frac{1}{2}}.\vec{n}_{j,k}}{f_j} \frac{\vec{q}_{j,k+\frac{1}{2}}}{|\, q_{j,k+\frac{1}{2}} \,|} \qquad (2)$$
where $d\vec{r}^{E}_{j,k} = (\vec{r}^{E}_{j,k+1} - \vec{r}_{j,k})$ and β is a relaxation parameter.

Choosing $\beta = 1$ will construct the grid along streamlines emanating from the contours. The first fraction reduces the growth in areas where the flow is non-orthogonal and the second fraction reduces the flow in zones where parts of the contour are close together.

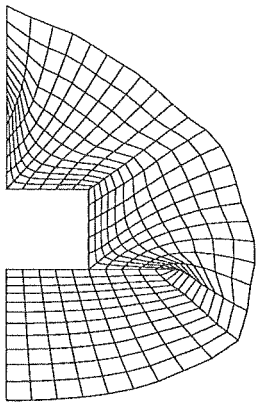

Figure 1: Grid generated with Panel grid generator: $\kappa = 0.0$.

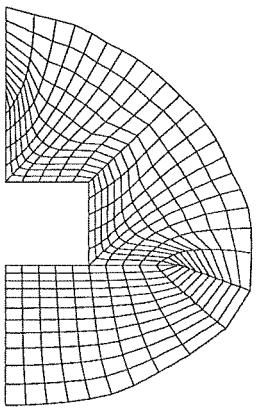

Figure 2: Grid generated with Panel grid generator: $\kappa = 0.5$.

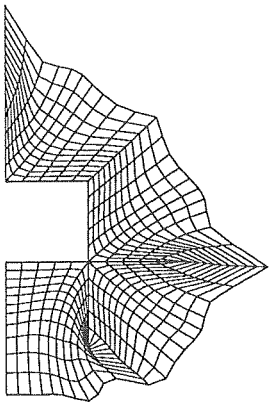

Figure 3: Grid generated with Panel grid generator: $\kappa = 0.0$.

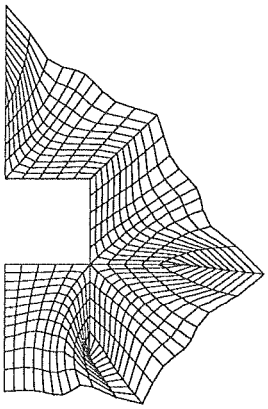

Figure 4: Grid generated with Panel grid generator: $\kappa = 0.5$.

This algorithm and its variants have been applied to several problems with concavities and their ability to prevent grid folding has been determined. Examples of 2-D grids generated with the method are shown in figures 1 to 4 about geometries which are symmetric with respect to the z-axis and only the part in the first and fourth quadrant are shown. The uneven figures shows results obtained with the Laplace equation ($\kappa = 0.0, \beta = 1.0$) and the even figures show results with the Helmholtz equation ($\kappa = 0.5, \beta = 1.0$). The main characteristic of the grids is the tendency to approximate very soon an equal arclength distribution. No grid folding in concave areas nor declustering in concave corners shows up and at the 360^o convex corners grid lines seem to cluster a bit with much skewness. It should be remembered that also the symmetric part of the configuration contributes to the grid directions which is felt particularly at the lower 360^o convex edge in figure 3 and 4. With respect to the κ damping term some small effects on grid folding and declustering are visible and a reasonable reduction of skewness can be noticed.

The aforementioned method has still a few drawbacks:

1. For some configurations the skewness might become too large. In which case the flow direction $\vec{q}$ of equation 2 should be limited.

2. In general, orthogonal grids cannot be generated with the Helmholtz equation and a panel method for other linear 'viscous' equations like the biharmonic one is then required.

3. The algorithm is explicit and might become unstable for some choices of grid spacing and growth.

4. The computational cost is equivalent to N^2,where N denotes the number of grid points on a contour. To reduce the cost,especially for 3-D applications, the method would need the embedding of multi-grid and clustering techniques [5]. Because accuracy and convergence requirements are much less restrictive in grid generation it should then be possible to make the computational cost closely equivalent to N. However,the development time is expected to be ¡ considerable.

Due to these drawbacks it was decided for 3-D grid generation to combine the panel grid generator method with a hyperbolic grid generator method which is described in the following section. The latter can generate orthogonal grids ,is implicit and efficient, but suffers from grid folding and declustering which can be prevented by the embedding of control by the panel grid generator.

3-D Hyperbolic grid generator with panel method control

The present 3-D hyperbolic grid generator follows closely the 2-D mathematical model as published in [3] and previous 2-D and 3-D work as published in [1, 2]. The present mapping from the computational space to the physical domain is based on the equations:

$$\frac{\vec{r}_\xi . \vec{r}_\zeta}{\mid r_\xi \mid\mid r_\zeta \mid} = \cos\phi \tag{3}$$

$$\frac{\vec{r}_\eta . \vec{r}_\zeta}{\mid r_\eta \mid\mid r_\zeta \mid} = \cos\theta \tag{4}$$

$$\mid \vec{r}_\xi . (\vec{r}_\eta \times \vec{r}_\zeta) \mid = V \tag{5}$$

Here (ξ, η and ζ) denote the coordinates of the computational space, θ and ϕ are the angle control terms first introduced in [3] for the 2-D problem.

The angles and the volume control term V are specified by the panel grid generator described earlier. For applications to slender transport type aircraft the assumption is made that θ and ϕ can be obtained in a quasi 3-D (strip theory method) way by application of the panel grid generator to 2-D transverse and longitudinal cross sectional reference contours. In the present work only two reference contours have been used:the 2-D transverse contour in the Trefftz plane $i = N_i$ and a 2-D longitudinal contour formed by the average x positions and the radius of equivalent circular contours having the same circumference as the grid contours i. In future work these data will be generated by a complete quasi 3-D panel method. For non-slender bodies which are not the subject of the present method a complete 3-D panel method might be needed.

Next the non linear equations (3) to (5) are linearized about the state $\vec{r}^0 = (x^0, y^0, z^0)^t$ resulting in the linear equation:

$$A\vec{r}_\xi + B\vec{r}_\eta + C\vec{r}_\zeta = \vec{f}$$

which can be written as the 3x3 hyperbolic system:

$$C^{-1}A\vec{r}_\xi + C^{-1}B\vec{r}_\eta + \vec{r}_\zeta = C^{-1}\vec{f} \tag{6}$$

where:

$$A = \begin{pmatrix} \frac{-\cos\phi^0 x^0_\xi}{|r^0_\xi|^2} + \frac{x^0_\zeta}{|r^0_\xi||r^0_\zeta|} & \frac{-\cos\phi^0 y^0_\xi}{|r^0_\xi|^2} + \frac{y^0_\zeta}{|r^0_\xi||r^0_\zeta|} & \frac{-\cos\phi^0 z^0_\xi}{|r^0_\xi|^2} + \frac{z^0_\zeta}{|r^0_\xi||r^0_\zeta|} \\ 0 & 0 & 0 \\ y^0_\eta z^0_\zeta - y^0_\zeta z^0_\eta & z^0_\eta x^0_\zeta - z^0_\zeta x^0_\eta & x^0_\eta y^0_\zeta - x^0_\zeta y^0_\eta \end{pmatrix},$$

$$B = \begin{pmatrix} 0 & 0 & 0 \\ \frac{-\cos\theta^0 x^0_\eta}{|r^0_\eta|^2} + \frac{x^0_\zeta}{|r^0_\eta||r^0_\zeta|} & \frac{-\cos\theta^0 y^0_\eta}{|r^0_\eta|^2} + \frac{y^0_\zeta}{|r^0_\eta||r^0_\zeta|} & \frac{-\cos\theta^0 z^0_\eta}{|r^0_\eta|^2} + \frac{z^0_\zeta}{|r^0_\eta||r^0_\zeta|} \\ y^0_\zeta z^0_\xi - y^0_\xi z^0_\zeta & z^0_\zeta x^0_\xi - z^0_\xi x^0_\zeta & x^0_\zeta y^0_\xi - x^0_\xi y^0_\zeta \end{pmatrix},$$

$$C = \begin{pmatrix} \frac{-\cos\phi^0 x^0_\zeta}{|r^0_\zeta|^2} + \frac{x^0_\xi}{|r^0_\xi||r^0_\zeta|} & \frac{-\cos\phi^0 y^0_\zeta}{|r^0_\zeta|^2} + \frac{y^0_\xi}{|r^0_\xi||r^0_\zeta|} & \frac{-\cos\phi^0 z^0_\zeta}{|r^0_\zeta|^2} + \frac{z^0_\xi}{|r^0_\xi||r^0_\zeta|} \\ \frac{-\cos\theta^0 x^0_\zeta}{|r^0_\zeta|^2} + \frac{x^0_\eta}{|r^0_\eta||r^0_\zeta|} & \frac{-\cos\theta^0 y^0_\zeta}{|r^0_\zeta|^2} + \frac{y^0_\eta}{|r^0_\eta||r^0_\zeta|} & \frac{-\cos\theta^0 z^0_\zeta}{|r^0_\zeta|^2} + \frac{z^0_\eta}{|r^0_\eta||r^0_\zeta|} \\ y^0_\xi z^0_\eta - y^0_\eta z^0_\xi & z^0_\xi x^0_\eta - z^0_\eta x^0_\xi & x^0_\xi y^0_\eta - x^0_\eta y^0_\xi \end{pmatrix}$$

and:

$$\vec{f} = \left(\cos\phi - \cos\phi^0, \cos\theta - \cos\theta^0, V + 2V^0\right)^t .$$

Finally equation (6) is integrated in ζ direction by the approximate factorization method:

$$\left[I + \alpha(C^{-1}A)_k\delta_\xi - \epsilon(\triangle\triangledown)^2_\xi\right] .$$

$$\left[I + \alpha(C^{-1}B)_k\delta_\eta - \epsilon(\triangle\triangledown)^2_\eta\right](\vec{r}_{k+1} - \vec{r}_k) = C^{-1}_k\vec{f}_k -$$

$$\left[(C^{-1}A)_k\delta_\xi - \epsilon(\triangle\triangledown)^2_\xi + (C^{-1}B)_k\delta_\eta - \epsilon(\triangle\triangledown)^2_\eta\right]\vec{r}_k \tag{7}$$

where k denotes the constant ζ contours and $\triangledown, \triangle$, and δ are backward,forward and central difference operators in η, ξ, respectively. C^{-1}, A, B, and $\vec{f}$ are calculated at the known k level. α is the implicitness parameter. Values of $\alpha > 1$ can be used to inhibit grid folding in concave zones. ϵ is the fourth-order dissipation parameter. Values of $\epsilon > 0$ can be used to smooth initial discontinuities. Extending [1], the right hand side of equation (7) is specified by functions with 'simple' shape and exponential growth or shrinkage:

$$V = \epsilon^k_c V^l + (1 - \epsilon^k_c)V^u_i$$

and:

$$\cos\theta = \epsilon^{k+1}_c(\cos\theta^b)_{k=0}$$

$$\cos\phi = \epsilon^{k+1}_c(\cos\phi^b)_{k=0}$$

where ϵ_c is the clustering (exponential) parameter, $V^u_i = \delta\xi_i(R_{k+1}+R_k)(R_{k+1}-R_k)\frac{\pi}{2N_j}$ is the volume of a uniform distribution in the far field ,R_k is the smallest radius of the equivalent circular bodies having the same circumference or volume as the grid contours $i = 0 \ldots N_i$ and $\delta\xi_i$ denotes the axial width of the cylinder strip i.

R_1 is obtained by letting each point i, j grow by $\min(\mid \vec{r}_\xi \mid, \mid \vec{r}_\eta) \mid)_{i,j,0}AR$ where AR denotes the average aspect ratio of the grid cells which has to be specified by the user. The other R_k's are determined for a completely convex surface k by:

$$R_{k+1} = R_k + (1+\epsilon_c)(R_k - R_{k-1})$$

and in other cases by:

$$R_{k+1} = R_k + \frac{(R_k - R_{k-1})R_k}{R_{k-1}} \quad .$$

The other volumes are determined by:

$$V^l = \epsilon_b \left(\frac{V^b}{V^s}\right)_{k=0} V^s + (1-\epsilon_b)V^s$$

$$\begin{aligned} V^s &= \epsilon_u \mid \vec{r}_\xi \times \vec{r}_\eta \mid_{j,k=0} \frac{(R_{k+1} - R_k)R_k}{R_0} \\ &+ (1-\epsilon_u) \mid \vec{r}_\xi \times \vec{r}_\eta \mid \min(\mid \vec{r}_\xi \mid, \mid \vec{r}_\eta) \mid)_{i,j,0} AR \end{aligned} \tag{8}$$

where ϵ_b is the BEM parameter. Values of $\epsilon_b > 0$ can be applied to activate the BEM grid generation algorithme to the $k = 0$ contour to prevent grid folding in concave zones and to concentrate grid lines somewhat in convex zones. The evaluation of $\cos\phi^b$,$\cos\theta^b$ and V_b is straightforward. ϵ_u is the uniformity parameter. A value of 1 produces contours at approximately equal distances while a value of 0 produces contours at approximately the contour spacing. The latter is less stable.

The 3x3 equations (7) are solved for each i and j contour by inverting a 13x(3x(N_i or N_j)) diagonal band matrix, first for all contours j and next for all contours i. Based on the aforementioned modelings a computer system BLOWUP has been developed for the generation of OH type meshes which consist of a preprocessor module which main task is the generation of the surface grid including the upwind slits (so-called diaphragmas) and downwind slits (wakes) and a grid generation module. Besides the abovementioned formulations the computer program has been designed such that the panel grid generation method can be invoked also from $k\#0$ grid contours which makes it possible to start with an orthogonal grid while limiting of V_s can be applied in concave areas. Also smoothing of the right hand side can be applied and finally post-elliptic smoothing with control functions [6] is embedded.

Quasi 3-D examples

Quasi 3-D grids about geometries with constant cross-sections in axial direction generated by the present method are presented for several geometries with concavities in figures 5-12. Figures 5 to 8 compare grids about geometries with moderate 90^o concavities obtained with the hyperbolic grid generator using a large amount of implicitness $\alpha = 3.0$ to prevent grid folding at the expense of losing orthogonality and clustering with grids obtained by using panel method control and $\alpha = 1.0$. The direction effects of the present grid generator are obvious. In general the present method prevents grid folding ,does not destroy the grid spacing in concave corners, clusters grid lines somewhat at convex corners and shows more skewness at 360^o convex corners. It should be noted that no attempts have been made to optimize the control parameters or the surface grid distributions in these examples to obtain a smoother grid.

Figure 9 to 12 show results about several geometries with strong concavities. It was not possible to obtain results without the panel method control by varying α, ϵ and ϵ_c! The uneven figures show plain results of the present method an the even figures show the grids after application of post-elliptic smoothing. The plain grid

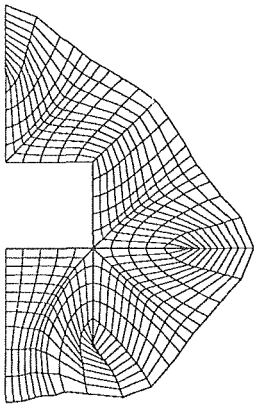

Figure 5: Grid generated with Hyperbolic grid generator with Panel method control:$\alpha = 1.0, \epsilon_u = 1.0, \epsilon = 0.1, AR = 0.5, \epsilon_c = 0.1, \epsilon_b = 0.3, \kappa = 0.0$

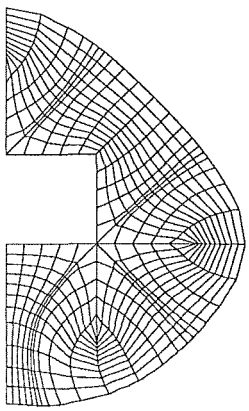

Figure 6: Grid generated with Hyperbolic grid generator with *no* Panel method control:$\alpha = 3.0, \epsilon_u = 1.0, \epsilon = 0.1, AR = 0.5, \epsilon_c = 0.1, \epsilon_b = 0.0, \kappa = 0.0$

of figure 9 is not smooth,has no grid folding and suffers from a significant amount of skewness. An undenyable improvement is obtained by applying elliptic smoothing afterwards. Also the plain grid of figure 11, about a geometry which probably is very close to the limits in applying the method is improved significantly after post-elliptic smoothing. It should be noted that no attempt has been made to adapt the surface distribution and the other control parameters α, ϵ and ϵ_c or to invoke the panel method at intermediate k planes.

The above quasi 3-D applications have shown the ability to generate grids about slowly varying slender shapes in axial direction and it can be concluded that the panel method control offers substantial benefits to the hyperbolic grid generator method. With respect to the skewness control a limiter has been recently embedded in the method.

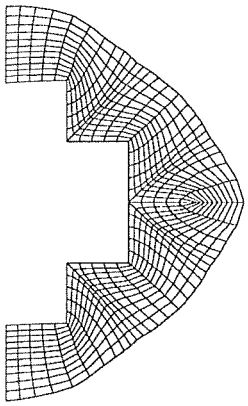

Figure 7: Grid generated with Hyperbolic grid generator with Panel method control:$\alpha = 1.0, \epsilon_u = 1.0, \epsilon = 0.1, AR = 0.5, \epsilon_c = 0.1, \epsilon_b = 0.3, \kappa = 0.0$

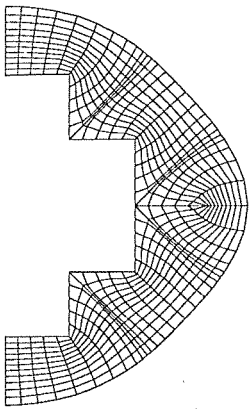

Figure 8: Grid generated with Hyperbolic grid generator with *no* Panel method control:$\alpha = 3.0, \epsilon_u = 1.0, \epsilon = 0.1, AR = 0.5, \epsilon_c = 0.1, \epsilon_b = 0.0, \kappa = 0.0$

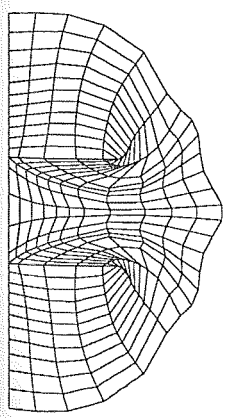

Figure 9: Grid generated with Hyperbolic grid generator with Panel method control:$\alpha = 1.0, \epsilon_u = 1.0, \epsilon = 0.1, AR = 0.5, \epsilon_c = 0.1, \epsilon_b = 0.8, \kappa = 0.0$.

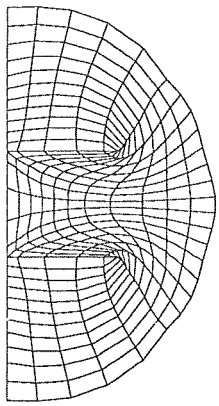

Figure 10: Grid generated with Hyperbolic grid generator with Panel method control:$\alpha = 1.0, \epsilon_u = 1.0, \epsilon = 0.1, AR = 0.5, \epsilon_c = 0.1, \epsilon_b = 0.8, \kappa = 0.0$ and using post elliptic smoothing

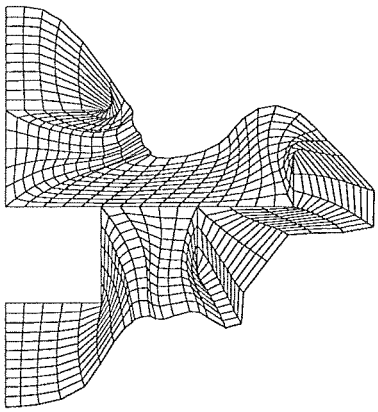

Figure 11: Grid generated with Hyperbolic grid generator with Panel method control:$\alpha = 1.0, \epsilon_u = 1.0, \epsilon = 0.1, AR = 0.5, \epsilon_c = 0.1, \epsilon_b = 0.8, \kappa = 0.0$

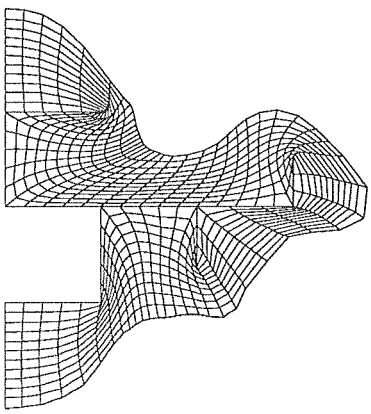

Figure 12: Grid generated with Hyperbolic grid generator with Panel method control:$\alpha = 1.0, \epsilon_u = 1.0, \epsilon = 0.1, AR = 0.5, \epsilon_c = 0.1, \epsilon_b = 0.8, \kappa = 0.0$ and using post elliptic smoothing

3-D examples

Also the investigation has been started to validate the grid generation method BLOWUP for configurations which have concavities in axial direction (airfoil and fuselage noses) and which have transverse cross-planes with varying sweep angles. The ability to generate 3-D grids about these configurations is demonstrated for several geometries in figures 13-30. Figures 13-18 show coarse grid data about a rectangular wing with NLR7301 airfoil sections. ¡ The examples were generated with the hyperbolic grid generator using a large amount of ¡ implicitness $\alpha = 3.0$ to prevent grid folding and also by using panel method control and $\alpha = 1.0$. The concavity at the blunt nose of the airfoil and also the convex double-valued corner at the tip cause no problems. The grid generated by using panel method control is the better one. Figures 19-24 show coarse grid data for a wing-body combination generated with the hyperbolic grid generator using the implicitness factor $\alpha = 3.0$ and also with panel method control and $\alpha = 1.0$. Figure 19 shows the input surface grid which is input to the geometry preprocessor of which the result, i.e. a surface grid distribution with upwind and downwind slits, is shown in figure 20. The concavity at the apex and at the wing-body junction and also the convex double-valued corners at the tip cause no problems. The grid generated with panel control is slightly better at the wing-fuselage junction. Finally figure 25-30 show coarse grid data about a T-tail-fuselage combination. In this case the tail surfaces have sweep angles which is reflected by the curvatures of the i grid planes. The examples were generated with the hyperbolic grid generator using $\alpha = 1.0$ and panel method control $\epsilon_b = 0.5$. From the above prelimenary 3-D applications it is concluded that the present hyperbolic grid generator method with panel method control is able to generate OH type grids around fairly complex shapes with concavities in a small turnaround time.

With respect to reduction of computational cost it is worthwhile to combine an algebraic grid generation scheme with the present method which can be used as soon as the concave zones are largely resolved by the present method.

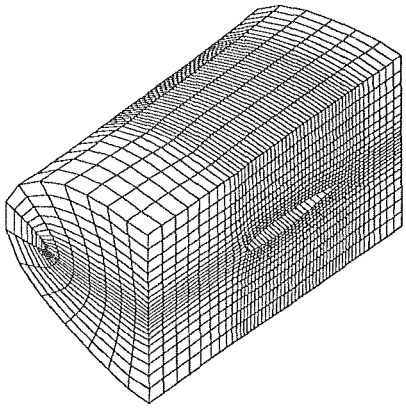

Figure 13: 3-D Grid part about a rectangular wing with NLR7301 airfoil sections generated by BLOWUP with control:$\alpha = 3.0, \epsilon_u = 1.0, \epsilon = 0.1, AR = 0.5, \epsilon_c = 0.2, \epsilon_b = 0.0, \kappa = 0.0$

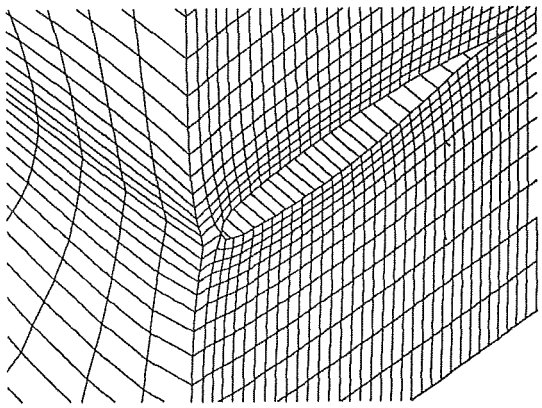

Figure 14: Close up at nose section of 3-D grid-part of figure 13

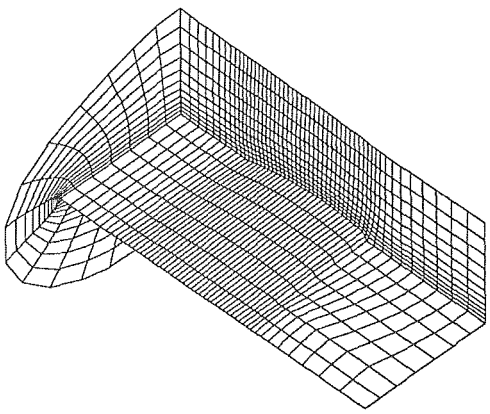

Figure 15: The same grid part as figure 13

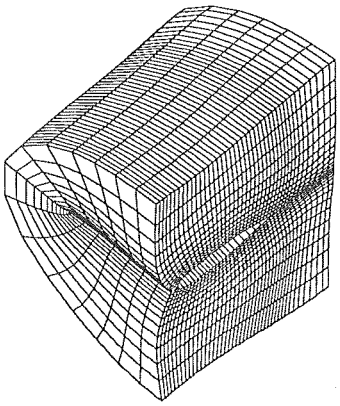

Figure 16: 3-D Grid part about a rectangular wing with NLR7301 airfoil sections generated by BLOWUP with panel method control:$\alpha = 1.0, \epsilon_u = 1.0, \epsilon = 0.1, AR = 0.5, \epsilon_c = 0.2, \epsilon_b = 0.5, \kappa = 0.5$

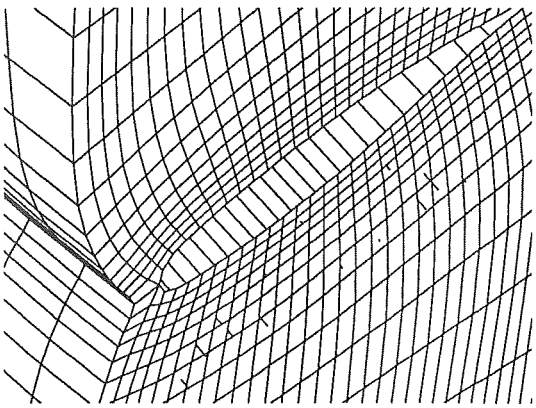

Figure 17: Close up at nose section of 3-D grid part of figure 16

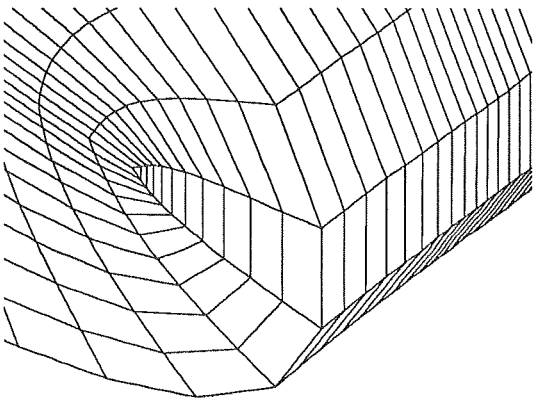

Figure 18: Close up at tip of 3-D grid-part of figure 13

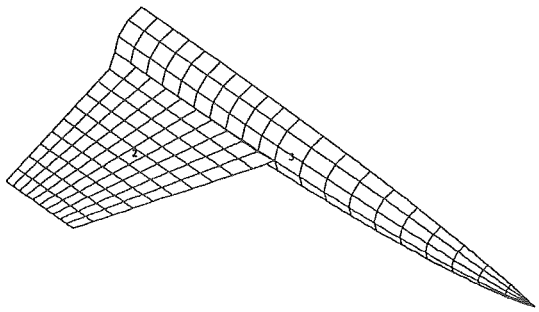

Figure 19: Input surface grid for preprocessor of BLOWUP for a wing body combination

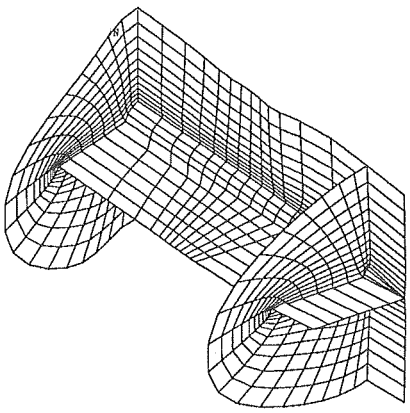

Figure 20: 3-D Grid about a wing-body combination generated by BLOWUP with control:$\alpha = 3.0, \epsilon_u = 1.0, \epsilon = 0.1, AR = 0.5, \epsilon_c = 0.1, \epsilon_b = 0.0, \kappa = 0.0$

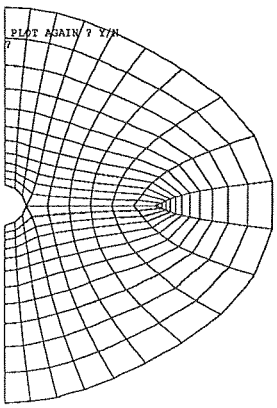

Figure 21: Transverse crossection of 3-D Grid part of figure 20

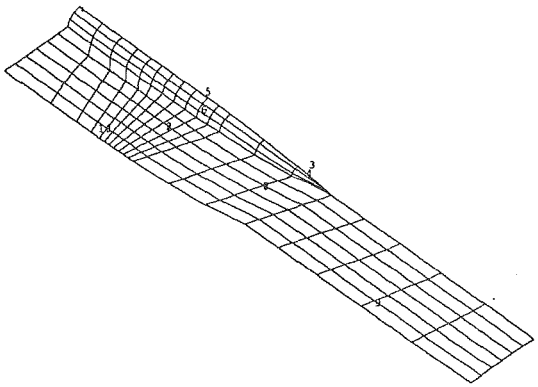

Figure 22: Surface grid with upwind and downwind slits for a wing body combination

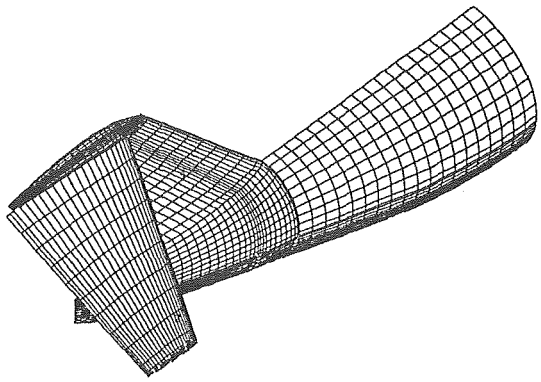

Figure 25: Input surface grid for preprocessor of BLOWUP for a T-tail-fuselage combination

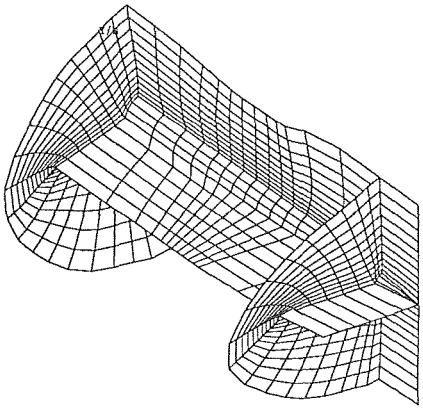

Figure 23: 3-D Grid about a wing-body combination generated by BLOWUP with panel method control:$\alpha = 1.0, \epsilon_u = 1.0, \epsilon = 0.1, AR = 0.5, \epsilon_c = 0.1, \epsilon_b = 0.5, \kappa = 0.5$

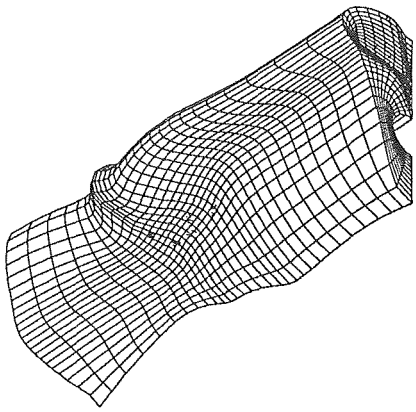

Figure 26: 3-D Grid part about a T-tail-fuselage combination generated by BLOWUP with control:$\alpha = 1.0, \epsilon_u = 1.0, \epsilon = 0.1, AR = 0.5, \epsilon_c = 0.1, \epsilon_b = 0.5, \kappa = 0.5$

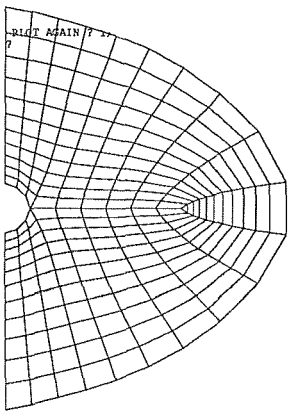

Figure 24: Transverse crossection of 3-D Grid part of figure 23

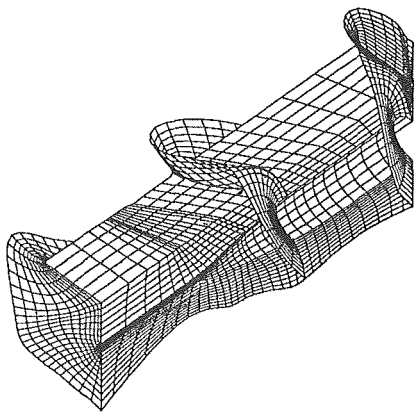

Figure 27: The same grid part as figure 26

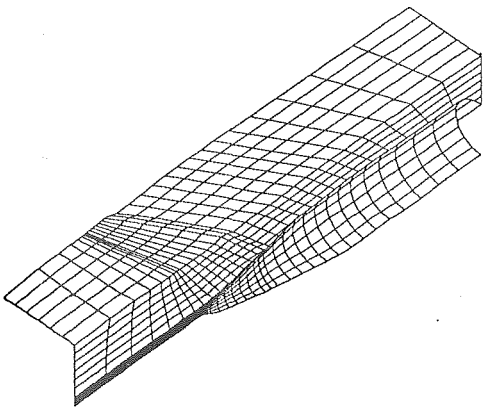

Figure 28: Surface grid with upwind and downwind slits for a T-tail-fuselage combination

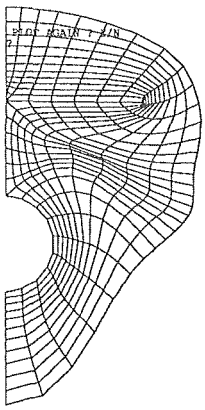

Figure 29: transverse cross-section of 3-D Grid generated with Hyperbolic grid generator about a T-tail-fuselage combination

Conclusion

A demonstration has been given of a panel method which is used to generate grids. The method has been embedded in a hyperbolic grid generator method to control grid folding and clustering in concave areas. The components of the method have been described and results of applications in 2-D and 3-D are shown.

It is concluded that the control by panel methods will reduce the effort to generate OH type grids around transport type aircraft with concavities by extending the applicability range, by improving grid quality and by a considerable reduction of turn-around time.

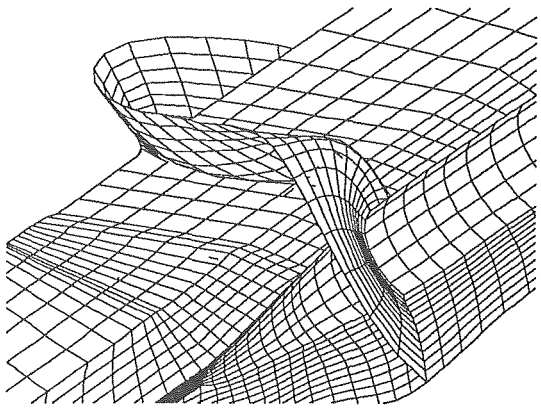

Figure 30: Close up at middle part of figure 27

Acknowledgement

This investigation was carried out partly under contract with the Netherlands Agency for Aerospace Programs(NIVR),contract number 01904N. Special thanks are due to Fokker Aircraft B.V. for providing the input data of the T-tail example.

References

[1] J.L. Steger et al. *Generation of body-fitted coordinates using hyperbolic partial differential equations*,SIAM J.Sci.Stat.Comput.,Vol. 1,No. 4, Dec. 1980, pp. 431-437

[2] J.L. Steger et al. *Generation of three -dimensional body-fitted coordinates using hyperbolic partial differential equations*,NASA TM 86753,June,1985

[3] J.Q. Cordova et al. *Grid generation for general 2-D regions using hyperbolic equations* ,AIAA-88-0520,Jan. 1988.

[4] M. H. L. Hounjet. *Hyperbolic grid generation with BEM source terms*,NLR TP 90334 U ,October 1990 also in Proceedings IABEM-90,Springer Verlag

[5] W. Hackbush et al. *On the fast matrix multiplication in the boundary element method by panel clustering*,Numer.Math.,Vol. 54,pp 463-491, 1989

[6] J. F. Thompson. *A general three-dimensional elliptic grid generation system on a composite block-structure*,Computer Methods in applied Mechanics and Engineering,Vol. 64,pp 377-411,1987